J Electroceram (2011) 27:120–125
DOI 10.1007/s10832-011-9656-5

Microwave and electrical behavior of Co^{2+} and Ru^{4+} ions substituted Ba-Sr sintered ferrite

Charanjeet Singh · S. Bindra-Narang · Inderjeet Singh Hudiara · K. Sudheendran · K. C. James Raju

Received: 3 December 2009 / Accepted: 22 September 2011 / Published online: 4 October 2011

Abstract The complex permittivity and complex permeability of synthesized M-type hexagonal ferrite powders, $Ba_{0.5}Sr_{0.5}Co_xRu_xFe_{(12-2x)}O_{19}$ (x=0.0, 0.2, 0.4, 0.6, 0.8, 1.0, 1.2) are measured at X-Band. The experimental results conclude that Co^{2+} and Ru^{4+} ions substitution enhances electromagnetic properties, rendering the use of ferrite for lossy applications. The acceleration in hoping mechanism between Fe^{2+} and Fe^{3+} ions leads to dominance of ε' and ε'' over μ' and μ'' along entire frequency band.

Keywords A-ceramics · D-dielectric properties · D-magnetic properties · D-electrical properties

1 Introduction

Electromagnetic pollution poses serious problem due to rapid development in wireless communication. Ferrites are being incorporated as shielding/absorbing materials to circumvent electromagnetic interference (EMI) and electromagnetic compatibility (EMC) problem at microwave frequencies [1, 2]. The pre-requisite for this is the attenuation of microwave signal depending upon dielectric and magnetic losses. Domain wall resonance in hexagonal ferrites is present towards lower end of microwave frequency spectrum and ferromagnetic resonance (FMR) at higher microwave frequencies. However FMR peaks are suppressed and permeability is reduced at microwave frequencies [3, 4]. The other option to enhance microwave attenuation is to increase dielectric losses through suitable substitution and sintering temperature.

In the previous paper, we reported static parameters of Co and Ru substituted Ba-Sr ferrite [5]. In the present paper for the first time, we have investigated electromagnetic properties of Ba-Sr hexagonal ferrite with substitution of divalent Co^{2+} ions and tetravalent Ru^{4+} ions and also suggested a composition for high frequency applications.

2 Experimental

Samples of M-type hexagonal ferrite, $Ba_{0.5}Sr_{0.5}Co_xRu_xFe_{(12-2x)}O_{19}$ (x=0.0, 0.2, 0.4, 0.6, 0.8, 1.0, 1.2), were prepared by Two Route Ceramic method [6]. Complex permeability (μ^*) and complex permittivity (ε^*) of samples were measured by using network analyzer (Agilent 8722ES) at 8.2–12.4 GHz using Nicholson-Ross method [7]. Calibration of the analyzer was made in air before carrying out final measurements, the entire frequency region was divided into 201 points i.e. readings were taken with successive increment of 0.021 GHz.

The procedure proposed by Nicholson-Ross method was deduced from the following equations

$$S_{11} = \frac{\Gamma(1 - T^2)}{(1 - \Gamma^2 T^2)} \quad (1)$$

C. Singh · S. Bindra-Narang · I. S. Hudiara
Department of Electronics Technology,
Guru Nanak Dev University,
Amritsar, Punjab, India

C. Singh (✉)
Department of Electronics and Communication Engg.,
Rayat-Bahra Institute of Engg. and Nanotechnology,
Hoshiarpur, Punjab, India
e-mail: charanjeet2003@rediffmail.com

K. Sudheendran · K. C. J. Raju
School of Physics, Central University Hyderabad,
Hyderabad, Andhra Pradesh, India

and

$$S_{21} = \frac{T(1-\Gamma^2)}{1-\Gamma^2 T^2} \tag{2}$$

Where Γ is the reflection coefficient and T is the transmission coefficient in a two port network.

These parameters can be obtained directly from the network analyzer.

The reflection coefficient can be deduced as

$$\Gamma = X \pm \sqrt{X^2-1} \tag{3}$$

$|\Gamma| < 1$ is used to find the exact root of this equation

$$X = \frac{S_{11}^2 - S_{21}^2 + 1}{2S_{11}} \tag{4}$$

$$T = \frac{S_{11} + S_{21} - \Gamma}{1-(S_{11}+S_{21})\Gamma} \tag{5}$$

The complex permeability is given as

$$\mu^* = \frac{1+\Gamma}{\Lambda(1-\Gamma)\sqrt{\frac{1}{\lambda_0^2}-\frac{1}{\lambda_c^2}}} \tag{6}$$

Where λ_0 is the free space wavelength and λ_c is the cut-off wavelength

and

$$\frac{1}{\Lambda^2} = \left[\frac{1}{2\pi L}\ln\left(\frac{1}{T}\right)\right]^2 \tag{7}$$

The complex permittivity is given as

$$\varepsilon^* = \frac{\lambda_0^2}{\mu}\left[\frac{1}{\lambda_c^2} - \left[\frac{1}{2\pi L}\ln\left(\frac{1}{T}\right)\right]^2\right] \tag{8}$$

here L is the thickness of the sample.

Resistivity was measured by two-probe method with Keithley setup 6517A [8].

3 Results and discussion

Structure characterization, using X-ray diffractograms and micrographs, has been explained in our previous investigation [5].

3.1 Complex permittivity and complex permeability

The substitution of Co^{2+} and Ru^{4+} ions increases dielectric constant (Fig. 1) in doped samples. The observed oscillatory behavior in ε′ is neither resonance nor relaxation type. Dielectric constant in ferrites after the applied field primarily depends on; space charge polarization emerging from electron displacement due to applied field, charge

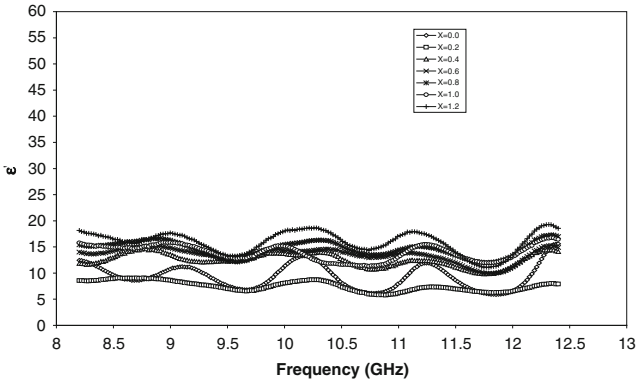

Fig. 1 Dielectric constant variation in $Ba_{0.5}Sr_{0.5}Co_xRu_xFe_{(12-2x)}O_{19}$ ferrite as a function of frequency and substitution (x=0.0,0.2,0.4,0.6,0.8,1.0,1.2)

formation at the grain boundary. Large ε′ in all the samples is ascribed to the formation of Fe^{2+} ions from Fe^{3+} ions at high sintering temperature of 1250°C, increasing electron hopping between Fe^{2+} and Fe^{3+} ions. A number of reports are available in the literature regarding the formation of Fe^{2+} ions from Fe^{3+} ions at high sintering temperature [9–13]. According to the Neel model, electron hopping between Fe^{2+} and Fe^{3+} ions is responsible for electric conduction and dielectric polarization [14].

Sample 0.2 shows lowest ε′ due to high resistivity (Log ρ, 8.2 Ω.cm) in Table 1, followed by sample 0.4 (Log ρ, 7.0 Ω.cm). High resistivity discourages polarization and conductivity [15], decreasing dielectric constant. Resistivity is inversely proportional to eddy current losses, a pre-requisite for high frequency applications to overcome these losses [11]. High resistivity in sample 0.2 makes it useful for wide frequency region. Sample 1.2 has high density and less porosity as shown in Fig. 2, increasing ε′ and ε″. On the other side it has high resistivity (Log ρ, 5.3 Ω.cm) than 1.0 (Log ρ, 4.0 Ω.cm) which will lower down ε′ and ε″. The competition between two factors increases ε′ and ε″ more in sample 1.2 than sample 1.0.

In M-type hexaferrite, Fe^{3+} cations occupy seven octahedral sites 12 k and 2a, trigonal site 2b with spins in one direction while two tetrahedral sites 4f2 and two octahedral sites 4f1 with spins in opposite directions [16]. Thus resistivity in ferrites primarily depends on octahedral sites with more strength than other sites and these

Table 1 Resistivity variation of $Ba_{0.5}Sr_{0.5}Co_xRu_xFe_{(12-2x)}O_{19}$ ferrite

x	Log(ρ) (Ω.cm)
0	5.6
0.2	8.2
0.4	7.0
0.6	5.7
0.8	4.4
1	4.0
1.2	5.3

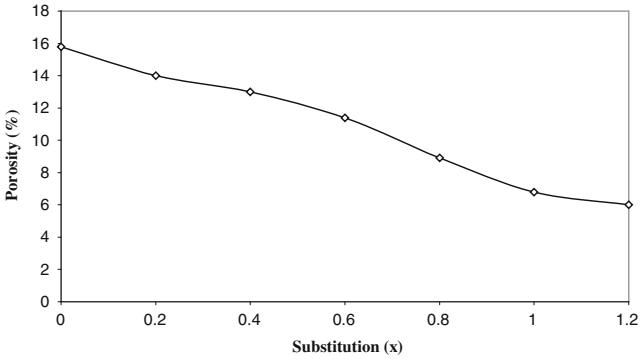

Fig. 2 Porosity variation in $Ba_{0.5}Sr_{0.5}Co_xRu_xFe_{(12-2x)}O_{19}$ ferrite as a function of substitution (x=0.0,0.2,0.4,0.6,0.8,1.0,1.2)

octahedral sites (B) are also large in comparison to tetrahedral sites (A) [17]. Ligand theory describes ions site occupancy on d-configuration and more electronegative ions tend to occupy B-site [18]. Ru^{4+} ions may occupy octahedral site due to large electronegativity (2.28) than Co^{2+} ions (1.88). While on other side, Ru^{4+} ions prefer to occupy A-site due to d^4 configuration and Co^{2+} ions B-site with d^7 configuration. Co^{2+} ions (0.72 Å) can also occupy B-site due to large ionic radius than Ru^{4+} ions (0.67 Å).

Different attributes for resistivity variation (Table 1) are explained as: The substitution of Ru^{4+} and Co^{2+} ions displaces Fe^{3+} ions from B to A site, increasing resistivity at lower substitution. Further substitution increases number of Fe^{3+} ions displacement. This increases the electron hopping between Fe^{2+} and Fe^{3+} ions, hence resistivity starts decreasing for $x>0.2$. However, resistivity increases at higher substitution (Table 1) attributed the preference of Co^{2+} ions for A-sites in addition to B-sites [19]. Thus, further substitution of Co^{2+} ions may displace Fe^{3+} ions from A to B sites, which presumably increases resistance at higher substitution.

Loss factor (Fig. 3) of doped samples almost increases with Co^{2+} and Ru^{4+} ions substitution. Dielectric loss mechanism of samples (except 0.2, 0.4) under consideration agrees with contributions from DC and AC conductivity or ion jump and dipole relaxation based on expression $\varepsilon'' = \left[(\sigma_{DC}/\omega\varepsilon_o) + \varepsilon''_{AC}\right]$, [20, 21]. Accordingly, dc conduction loss varies inversely with frequency, thus ε'' increases at low frequency region. Sample 0.2 and 0.4 show different oscillating behavior, ε'' remains at constant value (average) i.e. independent of frequency. Also ε'' remains low in sample 0.2 and 0.4 at most of frequencies as compared to other samples. This is ascribed to high resistivity than other samples (Table 1). The high value of ε'' in undoped sample 0.0 is due to the presence of maximum number of Fe^{2+} ions, which exchange electrons between Fe^{2+} and Fe^{3+} ions through hopping mechanism. Besides this, Fe^{2+} ions get easily polarized than Fe^{3+} ions leading to increase in loss factor. Sample 0.0 has significant dielectric loss at all frequencies unlike magnetic loss, which is nearly zero except in high frequency regime.

The comprehensive mechanism of complex permittivity is explained as: The substitution of the ferrites with the ions of different valencies will produce point like defects in the crystal lattice either in the form of vacancies or in the form of interstitials. We are substituting Co^{2+} and Ru^{4+} ions to the basic ferrite having Fe^{3+} ions in the present composition. This implies that we are replacing some of the Fe^{3+} ions with a less valence ion (Co^{2+}) which in turn results in an anionic vacancy, or with more valence (Ru^{4+}) ions, creating cationic vacancies. These vacancies will lower down the resistivity of the material and thereby enhancing the hopping conduction. The electronic hopping in the cationic and anionic vacancies will accelerate the dielectric losses. The presence of the defects/ionic vacancies will give more ionic nature to the bonding of the material which will result in increase of permittivity.

In this material system due to the high temperature processing (1250°C) there is also a possibility of formation of Fe^{2+} ions by the reduction of Fe^{3+} ion. The additional d electrons in the Fe^{2+} ions can travel to the neighboring Fe^{3+} as per the following mechanism.

$$Fe^{2+} + Fe^{3+} \leftrightarrow Fe^{3+} + Fe^{2+}$$

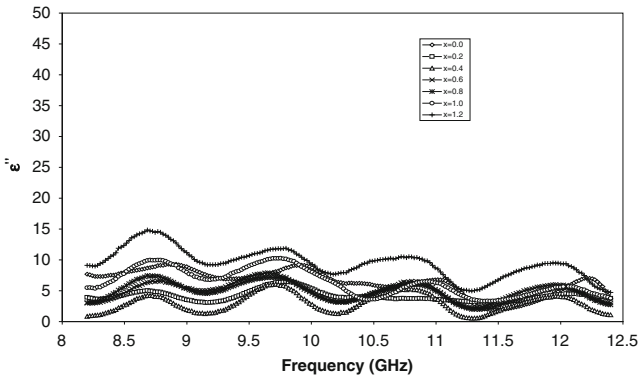

Fig. 3 Dielectric loss variation in $Ba_{0.5}Sr_{0.5}Co_xRu_xFe_{(12-2x)}O_{19}$ ferrite as a function of frequency and substitution (x=0.0,0.2,0.4,0.6,0.8,1.0,1.2)

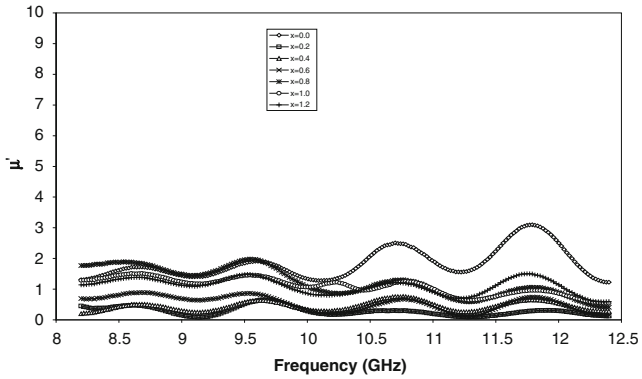

Fig. 4 Permeability variation in $Ba_{0.5}Sr_{0.5}Co_xRu_xFe_{(12-2x)}O_{19}$ ferrite as a function of frequency and substitution (x=0.0,0.2,0.4,0.6,0.8,1.0,1.2)

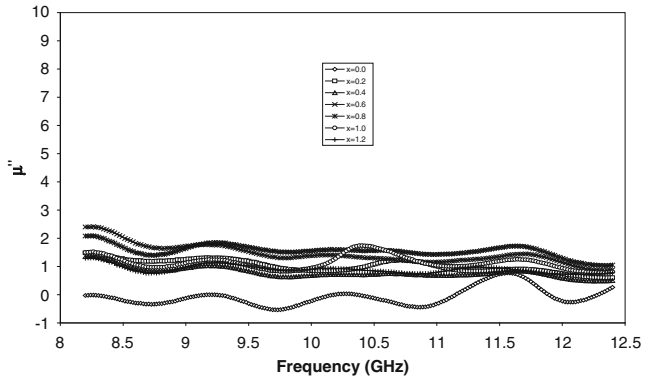

Fig. 5 Magnetic loss variation in $Ba_{0.5}Sr_{0.5}Co_xRu_xFe_{(12-2x)}O_{19}$ ferrite as a function of frequency and substitution (x=0.0,0.2,0.4,0.6,0.8,1.0,1.2)

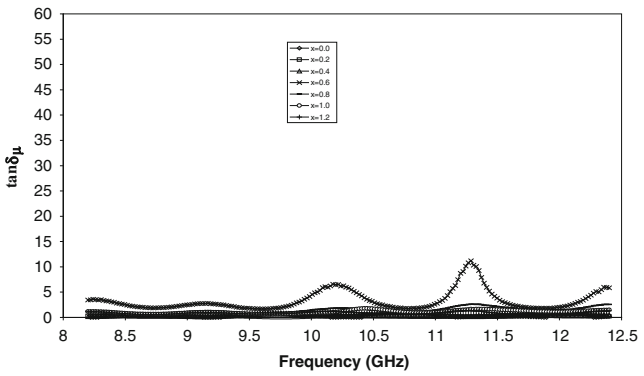

Fig. 7 $\tan\delta_u$ variation with frequency and substitution in $Ba_{0.5}Sr_{0.5}Co_xRu_xFe_{(12-2x)}O_{19}$ ferrite (x=0.0,0.2,0.4,0.6,0.8,1.0,1.2)

This hopping of electrons results in increase of dielectric loss. As explained earlier, these Fe^{2+} ions are easily polarized than Fe^{3+} ions causing increase in ε′ and ε″.

Permeability dispersion (Fig. 4) of undoped sample 0.0 exhibits ambiguous increase with frequency. In doped samples, μ′ increases with Co and Ru ion substitution. μ′ is large at high substitution as compared to low substitution and decreases fast with frequency at higher substitution. Sample 0.2 shows minimum permeability almost at all the frequencies. The above variations cannot be attributed to particular reason.

The magnetic loss arises due to lag between magnetization and applied field. The substitution of Co^{2+} and Ru^{4+} ions causes increase in grain size [5] and increase in density. This further enhances domain wall mobility, increasing μ″ in doped samples (Fig. 5). μ″ decreases non-linearly in doped samples from low to high frequency regime and this effect is more pronounced in sample 0.6 and 0.8. Thus, the complex permeability does not reflect significant variation in comparison to the complex permittivity.

Sample 0.4 shows large $\tan\delta_\varepsilon$ (Fig. 6) over entire frequency regime while other samples have comparatively low values. Both $\tan\delta_\mu$ (Fig. 7) and $\tan\delta_\varepsilon$ vary with frequency, and $\tan\delta_\varepsilon$ is higher than $\tan\delta_\mu$ in all samples at entire X-band.

4 Oscillatory behavior of μ* and ε*

The hexagonal ferrites manifest an oscillatory behavior in their dielectric and magnetic properties. The dielectric properties of Ba-Co and Ba-Mn-Ti hexagonal ferrites were reported by Meshram et al. at X band frequencies [22]. These samples revealed the oscillatory behavior for both dielectric and magnetic properties. Recently, complex permeability and permittivity of barium based M-type hexagonal ferrites were reported by Abbas et al. [23]. They also observed oscillatory behavior, similar to our results, in complex permittivity and complex permeability. They attributed the behavior of dielectric properties to the difference in relaxation frequencies of various dipoles. The oscillatory behavior of magnetic properties was explained in terms of the interactions of the magnetic vector with microwaves and the change in direction of the magnetic vector due to substitution.

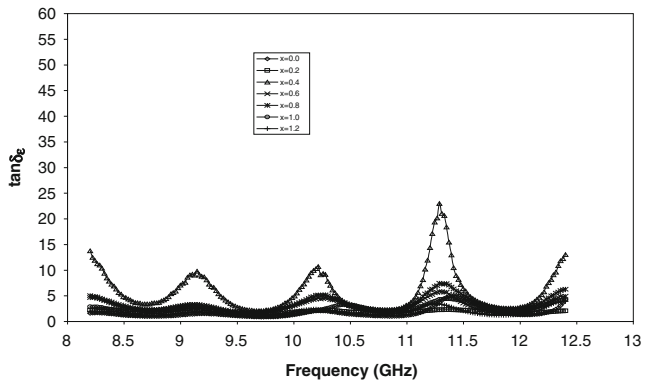

Fig. 6 $\tan\delta_\varepsilon$ variation with frequency and substitution in $Ba_{0.5}Sr_{0.5}Co_xRu_xFe_{(12-2x)}O_{19}$ ferrite (x=0.0,0.2,0.4,0.6,0.8,1.0,1.2)

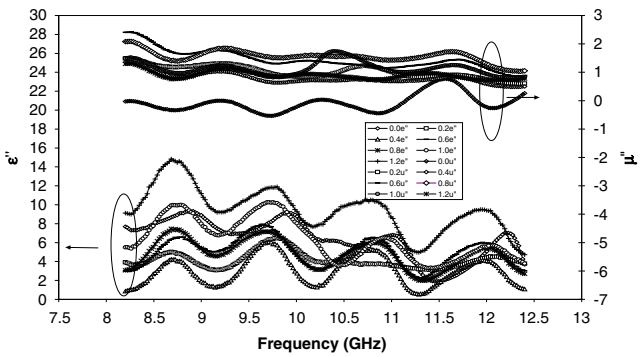

Fig. 8 Anti-phase oscillations of magnetic loss and dielectric loss in $Ba_{0.5}Sr_{0.5}Co_xRu_xFe_{(12-2x)}O_{19}$ ferrite (x=0.0,0.2,0.4,0.6,0.8,1.0,1.2)

In the present experiment compounds are having a variety of positive ions of different valancies and have different co-ordination with O^{2-} ions as reported a by Abbas at el. [23]. Hence, dipoles of various strengths are formed in the same material. These different dipoles have different relaxation frequencies. The electron hopping between Fe^{3+} and Fe^{2+} ions will give rise to another relaxation. Among the different relaxation mechanisms of various dipoles formed in the ferrite material, hopping of the electrons and the relaxation characteristics (space charge polarization) together could be responsible for the oscillatory behavior of the dielectric properties. The oscillatory behavior of the magnetic loss can be explained in terms of the precision motion of the magnetization vector. In M-type hexagonal ferrites the 12 Fe^{3+} ions are distributed in three different interstitial sites viz. tetragonal, octahedral and bi-pyramidal. The seven octahedral ions and one bi-pyramidal ions are oppositely coupled with two octahedral ions and two tetrahedral ions giving a net magnetization of only 4 Fe^{3+} ions. The magnetization vector on interaction with microwave signal should produce stable resonances. But due to the substitution of cobalt and ruthenium, the magnetization vector will be shifted more towards the base line and hence its interaction with the microwave field results in a zig zag or oscillatory variation of the magnetic properties. Referring to Figs. 1, 3, 4, 5, 6 and 7 it could be stated that the sample responses vary with the composition, other parameters like sample thickness and measurement conditions are identical for all the samples.

Moreover, a slight oscillation in the measured data can arise from the measurement procedure. It is widely accepted that the Nicholson Ross method, used here to determine complex permittivity and permeability, shows a divergence at frequencies corresponding to integral multiples of half wavelength in the sample. Here the complex transmission T and the reflection coefficient Γ are calculated from the S parameter measurements. Nicholson and Ross assumed an infinitely thick sample to take into account the behavior of the reflection coefficient. Reflection coefficient is an oscillatory function of layer thickness with periodic oscillations at every half wavelength [24]. In the case of absorbing materials, the amplitude of oscillation increases with the decrease of sample thickness. When the sample is infinitely thick, the refection coefficient becomes constant. In the present study, the Nicholson Ross method was used only to calculate the T in terms of the measured Γ and complex permittivity, permeability. This approach cannot eliminate the effect of oscillatory behavior of the complex reflection coefficient in the dielectric and magnetic properties as long as the samples are of finite thickness.

The frequency dependence of imaginary permeability exhibits anti-phase oscillations with imaginary permittivity (Fig. 8) from 8.2 GHz to 12.4 GHz. So the total loss (dielectric + magnetic) does not oscillate with frequency, concluding that oscillations in μ'' and ε'' (also in μ' and ε') are due to measurement uncertainty and apparent splitting is ascribed to the measurement error. Negative values of μ' (X-Band) and $\tan\delta_\varepsilon$ (0–40 GHz) have also been reported earlier [25–27].

Therefore, the observed oscillatory behavior in the complex permittivity and permeability can be considered as a combined behavior of material properties and the measurement procedure itself.

5 Conclusions

This first ever investigation on Co-Ru substituted Ba-Sr ferrites concludes that microwave attenuation is possible by increasing dielectric losses through appropriate sintering temperature and substitution, while in previous reports magnetic properties are enhanced to achieve microwave attenuation. Hopping mechanism and resistivity account for dielectric constant and dielectric loss variation. The dielectric properties are enhanced in comparison to magnetic properties. Large $\tan\delta_\varepsilon$ in sample 0.4 suggests for lossy applications at high frequencies.

References

1. H.-S. Cho, S.-S. Kim, IEEE Trans Magn **35**, 3151 (1999)
2. V.K. Varadan, V.V. Varadan, W.F. Hall, IEEE Trans Microwave Theory Tech **34**, 251 (1986)
3. C.E. Patton, Microwave resonance and relaxation, in *Magnetic oxides*, ed. by D.J. Craik (Wiley, London, 1975), p. 575
4. E.E. Riches, *Ferrites: A Review of Materials and Applications* (Mills and Boon, London, 1972)
5. C. Singh, S. Bindra-Narang, I.S. Hudiara, Y. Bai, F. Tabatabaei, Mater Res Bull **43**, 176 (2008)
6. A.J. Goldman, *Handbook of Modern Ferromagnetic Materials* (Kluwer, 1999)
7. A.M. Nicolson, G.F. Ross, IEEE Trans Instrum Meas **IM-19**, 377 (1970)
8. V.R.K. Murthy, J. Sobhanadri, Phys Status Solidi A **38**, 647 (1976)
9. N. Gupta, M.C. Dimri, S.C. Kashyap, D.C. Dube, Ceram Int **31**, 171 (2005)
10. L.G. Van Uitert, J Chem Phys **23**, 1883 (1955)
11. A. Verma, R. Chatterjee, J Magn Magn Mater **306**, 313 (2006)
12. J.M. Brownlow, J Appl Phys **29**, 373 (1958)
13. J. Bao, J. Zhou, Z. Yue, L. Li, Z. Gui, J Magn Magn Mater **250**, 131 (2002)
14. A.M. Abdeen, J Magn Magn Mater **192**, 121 (1999)
15. A.K. Singh, A. Verma, O.P. Thakur, C. Prakash, T.C. Goel, R.G. Mendiratta, Mat Lett **57**, 1040 (2003)

16. D. Lisjak, M. Drofenik, J Eur Ceram Soc **24**, 1841 (2004)
17. M.V. Rane, D. Bahadur, S.D. Kulkarni, S.K. Date, J Magn Magn Mater **195**, L256 (1999)
18. A. González-Angeles, G. Mendoza-Suárez, A. Grusková, J. Lipka, M. Papánová, J. Sláma, J Magn Magn Mater **285**, 450 (2005)
19. Z. Šimša, S. Lego, R. Gerber, E. Pollert, J Magn Magn Mater **140–144**, 2103 (1995)
20. V.T. Truong, S.Z. Riddell, R.F. Muscat, J Mater Sci **33**, 4971 (1998)
21. A.K. Jonscher, in *Dielectrics Relaxation in Solids* (Chelsea Dielectric, London 1983), p. 46
22. M.R. Meshram, N.K. Agrawal, B. Sinha, P.S. Misra, J Magn Magn Mater **71**, 207 (2004)
23. S.M. Abbas, A.K. Dixit, R. Chatterjee, T.C. Goel, J Magn Magn Mater **309**, 20 (2007)
24. Z. Abbas, R.D. Pollard, R.W. Kelsall, IEEE Trans Microwave Theory Tech **46**, 2011 (1998)
25. F. Brown, C.L. Gravel, J Phys Rev **97**, 55 (1955)
26. W.H. Von Aulock, *Handbook of Microwave Ferrite Materials* (Academic, London, 1965)
27. M.D. Janezic and Williams, D.F., IEEE Int Microwave Symp Digest, (1997) 1343.